

Laser Photolysis of Silver Colloid Prepared by Citric Acid Reduction Method

Alexander Pyatenko,* Munehiro Yamaguchi, and Masaaki Suzuki

Research Institute of Genome-based Biofactory, National Institute of Advanced Industrial Science and Technology (AIST), Sapporo 062-8517, Japan

Received: September 16, 2005

By irradiating a silver colloid, prepared via the citric reduction method, using the second harmonic of a Nd:YAG laser, $\lambda = 532$ nm, with laser fluence more than about 0.2 J/cm^2 , we prepared a colloid consisting of small spherical silver nanoparticles with $d_p = 8$ nm. The process of particle formation can be divided into three steps. First, large particles that existed in the initial colloid evaporate fully, producing a large amount of silver atoms. Next, primary particles with $d_p = 2\text{--}4$ nm are formed in mini plumes. Finally, these primary particles grow up to 8 nm, as silver atoms diffuse to them through water.

Introduction

Silver nanoparticles are very attractive for biophysical, biochemical, and biotechnological applications due to their unusual physical properties, especially due to their sharp plasmon absorption peak.^{1,2} Of the many different existing methods of preparation of such particles, the most simple and most commonly used bulk-solution synthesis method is chemical reduction of metal salt. Compared to gold, silver particles produced by this method are relatively large and have a wider size distribution. Alternatively, nanosecond laser ablation of a metal surface immersed in a liquid has recently been used for synthesis of nanoparticles of different noble metals.^{4–7} A more precise understanding of the ablation mechanism is necessary to better control the particle size. This process is very complicated and consists of target heating, melting, and ablation steps, as well as post-irradiation of ablated particles in the colloid by the following laser pulses. This last post-irradiation step has been studied only little until now.

On the other hand, several papers have shown that laser irradiation of colloidal nanoparticles can reduce their size. The possibility of such size reduction for silver nanoparticles was demonstrated by Kamat et al.³ The authors irradiated silver colloid prepared with citric reduction method using the third harmonic of Nd:YAG laser ($\lambda = 355$ nm) with beam diameter of about 5 mm and pulse energy of 1.5 mJ. After 3 min of irradiation the particle size reduced from the original 40–60 nm to 5–20 nm. For an explanation of their results, the authors of ref 3 proposed the scheme of particle fragmentation. According to their model, transient aggregates were formed via the photoejection of electrons into the solvent. The size reduction of gold nanoparticles was studied in more detail by Takami et al.⁸ They demonstrated high efficiency of particle size reduction using the second harmonic of Nd:YAG laser ($\lambda = 532$ nm) and explained the experimental results using a simple model, assuming that the laser energy absorbed by a particle in the colloid went into particle heating, melting, and vaporization.

The purpose of this research was to study the detailed mechanism of silver particle size reduction during the irradiation of a silver colloid, prepared with standard citric reduction method, using a nanosecond pulse laser.

Experimental Section

The initial colloid was prepared by the citric reduction method.⁸ A 50 mL portion of 0.01 M AgNO_3 was added to 450 mL of double distilled water and then heated via stirring to achieve boiling. A 1 g portion of trisodium citrate, $\text{C}_6\text{H}_5\text{Na}_3\text{O}_7$, was dissolved in 100 mL of water. Just as boiling began, 10 mL of this citrate solution was added. Boiling then continued for 1 h. After about 3 min of boiling, the solution turned yellow, and after about 5 min it turned gray-yellow and became opaque. The extinction spectrum of this initial colloid diluted 10 times with water is shown in Figure 1 (curve a). The peak shape and position clearly shows that the colloid was composed of large, nonspherical particles. The results of TEM observation, shown in Figure 2, proved that the main component of the colloid was large spheroid particles with typical size of about 120 nm and an aspect ratio of about 1.5. Apart from these particles, a relatively large amount of nanorods with different lengths and thicknesses were observed. TEM results did not depend on the colloid dilution factor.

A 5 mL sample of this colloid was then placed in a small glass vial of 20 mm diameter and was irradiated by the second harmonic of a Nd:YAG laser ($\lambda = 532$ nm). The diameter of the laser beam was 7 mm. Pulse duration was about 10 ns, and pulse frequency was 10 Hz. Maximum laser power was 3 W, which corresponds to maximum laser fluence, $J = 0.78 \text{ J/cm}^2$. Immediately after the irradiation experiment, the UV–vis absorption spectra were measured by a Shimadzu UV-1200 spectrometer, and samples for TEM observation were prepared by dropping the colloid onto a carbon–copper grid, and then left to dry for 1 day at room temperature.

Results

While the original colloid was opaque, the same colloid became optically transparent, dark yellow in color, after irradiation. These yellow colloids were usually stable for several months. The UV–vis extinction spectrum of a colloid irradiated with laser power of 3 W for the duration of 30 min is shown in Figure 1 (curve b). Because the intensity of the absorption peak was too high, irradiated colloid had to be diluted with water in 1:10 ratio. In this case, the main characteristics of the plasmon peak (position of maximum, $\lambda_{\text{max}} = 392$ nm, and peak width, FWHM = 39 nm) remained the same, with λ_{max} range of ± 2

* Corresponding author. E-mail: alexander.pyatenko@aist.go.jp

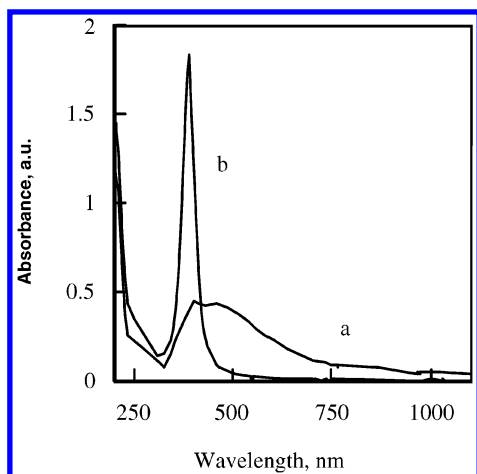


Figure 1. UV-vis extinction spectra for (a) initial colloid prepared with citric reduction method; (b) same colloid after irradiation with laser power 3 W for 30 min. Both colloids were diluted with water in 1:10 ratio before measurements.

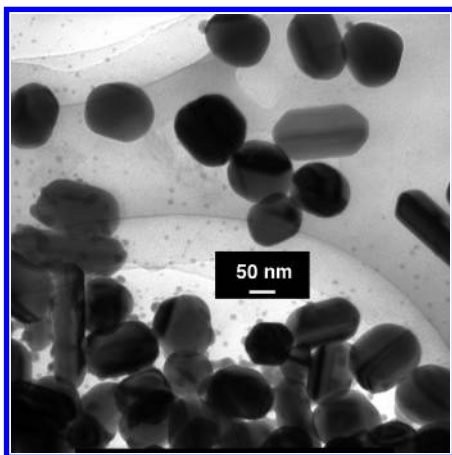


Figure 2. Typical TEM image of initial silver colloid.

nm and FWHM range of ± 3 nm, for laser power of 1–3 W and irradiation duration of 10–30 min. The same results were obtained when the initial colloid was preliminary diluted with water in 1:10 ratio and then irradiated. Using citrate/water solution, with different citrate concentrations for dilution, shifted the plasmon peak into the red region by 4–6 nm and widened the peak by 5–10 nm.

To study the time dependence of the plasmon peak, we diluted the initial colloid with water in 1:10 ratio and irradiated it for various lengths of time, varying the laser power. The results for λ_{max} and FWHM are shown in Figure 3. Both values changed very specifically with irradiation time. The time dependences for both values strongly depended on the laser fluence. For relatively high laser fluences, $J > 0.18$ J/cm², the plasmon absorption peak became rather narrow (FWHM of about 45–50 nm), and the maximum position approached a constant value during the first 30–60 s. After that, both characteristics decreased very slowly during the next 5–10 min. For relatively low laser fluences, the plasmon peak remained rather wide, and its maximum position was shifted into the red for a long time. Such behavior of the plasmon absorption peak showed clearly that the process of particle size reduction is very different for high and low laser fluences. The boundary value for laser fluence is about 0.18 J/cm².

A typical TEM image produced for a colloid irradiated with laser power of 3 W for 30 min is shown in Figure 4. The particles are very spherical and very homogeneous. Some of

the particles exhibited the surface pattern typical of polycrystalline. Electron diffraction patterns also confirmed the polycrystalline nature of these particles. The relative diameters of diffraction rings coincided within 2–5% with those calculated using the references values for silver interplanar spaces.¹⁰ The inset in Figure 4 shows the histogram of particle size distribution. This histogram corresponds to the average particle size of $d_p = 8.1 \pm 1.7$ nm. These 8 nm particles were observed for a wide range of experimental conditions: laser power ranging 1–3 W and irradiation duration of 5–60 min. Apart from these “small” particles, very small particles with size of 2–4 nm were observed. Although the total amount of these “very small” particles was much lower than that of the “small” ones, certain parts of the meshes were completely covered by them.

Discussion

All the results presented above could be explained by the particle heating, melting, and vaporization model, proposed by Takami et al.,⁸ to explain the reduction in the size of gold particles after irradiation by nanosecond Nd: YAG laser pulses. According to this model, the heat loss processes is considered to be negligible compared to the energy absorbed by the particle while irradiated by the laser pulse, and the total absorbed energy is then transformed to particle heating, melting, and vaporization. All three processes are very fast and complete within the time period between two consecutive laser pulses, 100 ms.

The energy absorbed by a particle irradiated by a single laser pulse is equal to

$$Q_{\text{abs}} = J \sigma_{\text{abs}}^{532} \quad (1)$$

where J is the laser fluence, and $\sigma_{\text{abs}}^{532}$ is the absorption cross section of the particle for a given wavelength, i.e., 532 nm in our case.

There are no reliable experimental data on absorption cross sections. Moreover, in simulation, people calculate the extinction rather than absorption cross section, which is the sum of absorption and scattering. The extinction spectra, $\sigma_{\text{ext}}(\lambda)$, were calculated by Jensen et al.¹¹ for six different sizes of silver nanoparticles. Later, the same research group showed how two components of extinction, absorption and scattering, changed between small and large gold nanoparticles.¹² For gold particles with a diameter smaller than 50 nm, scattering is negligible and extinction is practically equal to absorption. For gold particles with $d_p = 200$ nm, the situation changes dramatically, and scattering dominates (at wavelength of 532 nm). Due to the lack of data, we assumed the same ratios between the extinction and absorption for silver particles, and by using the extinction data from ref 11 estimated the absorption cross section at 532 nm for silver nanoparticles of different sizes. Using this estimation, we were able to calculate the energy absorbed by the particle (1), and by using the simple energy balance equation

$$Q_{\text{abs}} = \rho_p (\pi d_p^3 / 6) (c_p \Delta T + \Delta H_m + \Delta H_v) \quad (2)$$

to calculate for particles of different size, d_p , the minimum laser fluence, J_0 , required to heat a particle up to the boiling point, $T_b = 2212$ °C, complete melting, and vaporization by one laser pulse. All physical and thermodynamical constants used in eq 2, i.e., silver density, ρ_p , and heat capacity, c_p , heat of melting, ΔH_m , and heat of vaporization, ΔH_v , were adopted from Perry.¹³

Such calculated minimum laser fluence is shown in Figure 5 as a function of particle diameter. It can be seen from Figure 5 that, by working with laser fluence 0.8 J/cm², it is possible to

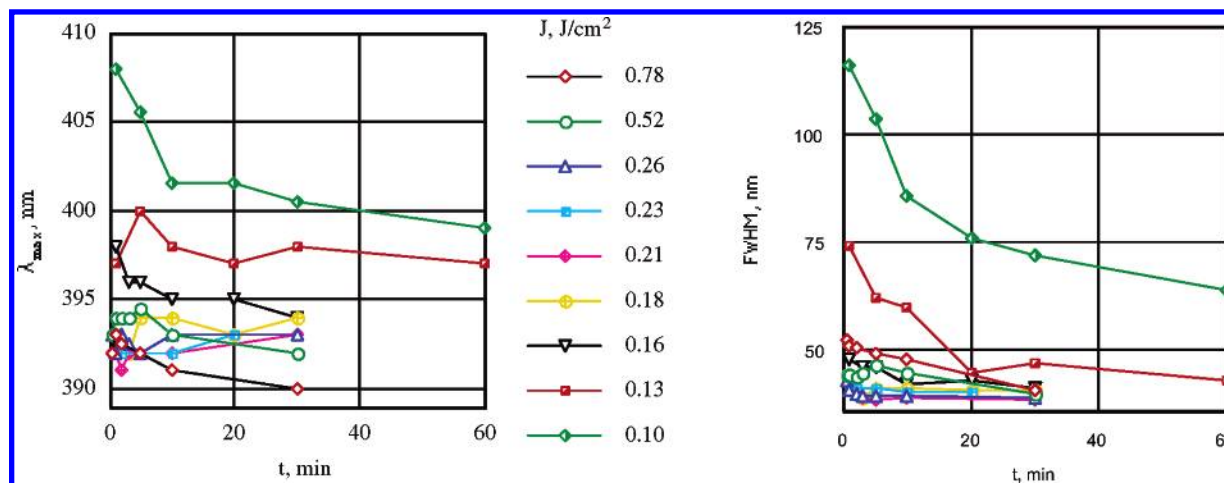


Figure 3. Time dependence of the two main characteristics of the surface plasmon peak: position of peak maximum, λ_{\max} , and peak width, FWHM, for different laser fluences.

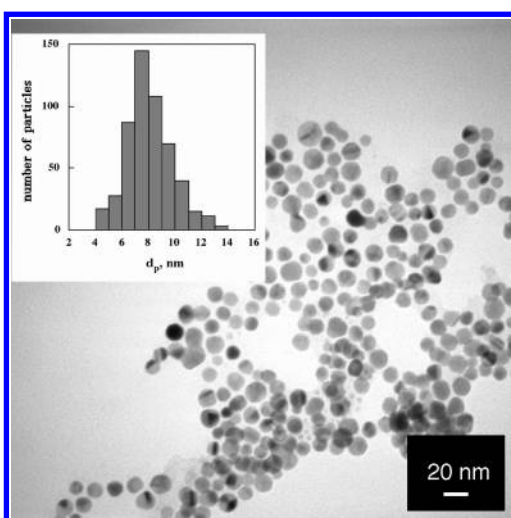


Figure 4. Typical TEM image of silver colloid irradiated with laser power 3 W for 30 min. Inset shows the histogram for particle size distribution.

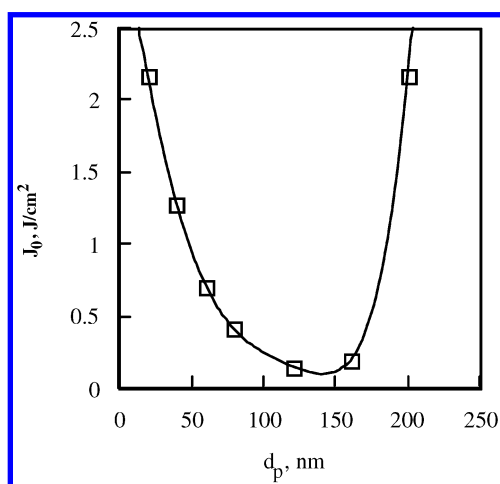


Figure 5. Minimum laser fluence, J_0 , needed for particle heating, melting, and complete vaporization by one laser pulse, as a function of particle diameter.

evaporate completely, using a single laser pulse, all particles in size range of 55–180 nm. However, for laser fluence of 0.15 J/cm², this size range decreases to 125–150 nm. And if the laser fluence is lower than 0.08 J/cm², no particle could be evaporated completely by a single laser pulse. For complete

evaporation of primary colloid particles with average size of about 120 nm, a minimum fluence of about 0.16 J/cm² is necessary. This value is very close to the boundary between high and low laser fluences, 0.18 J/cm², which can be observed in Figure 3. It can be pointed out that the above estimations of minimum fluences were made for naked silver particles, while the measurements of the plasmon peak time-dependence, presented in Figure 3, were performed for silver particles covered by a citrate layer. The citrate layer has to increase the particle absorption cross section.² However, taking into account the results for different dilution factors (with water or citrate), we believe that the absolute increase in $\sigma_{\text{abs}}^{532}$ value is not very large.

Finally, the process of laser photolysis of silver colloid could be ascribed as following: for relatively large laser fluences, $J > 0.18$ J/cm², all particles that met with the laser beam were vaporized completely. Inside of the hot, dense cloud of silver atoms (plume), small embryonic particles were formed thru mutual collisions between silver atoms. According to our TEM results, the size of these embryonic particles was about 2–4 nm. The embryonic particles then grew relatively slowly, while collecting free silver atoms, which diffused to them through water. The final particle size was 8 nm. These 8 nm particles were completely covered by a citrate layer that prevented further particle growth and agglomeration. If laser fluence is smaller than 0.18 J/cm², the primary particles will be only partially evaporated by a laser pulse, and some core part of each particle will remain. But, in such partial vaporization process, the particle will completely loose the surrounding citrate layer protecting the particle from further growth. Because a lot of silver atoms are produced in the vicinity, the core of the particle could grow as the surrounding atoms diffuse to it through the water. This last process of particle growth will be different for different particles, depending on the core size, local concentration of silver atoms, and the lifetime of a particular core, so that some of the cores could potentially grow to become even larger than the original particle. Thus, for relatively low laser fluence, two competing processes of partial particle vaporization and subsequent core growth, will take place. This competition between particle growth and vaporization was responsible for the slow changes of the plasmon peak that we observed for relatively low laser fluences ($J < 0.18$ J/cm²).

According to our estimations 8 nm particles will also undergo partial vaporization, and thus, will loose their protective citrate layer in each laser irradiation act. However, because of the small

absorption coefficient, the amount of silver evaporated from this particle will be smaller than 20% of the particle mass. Thus, the local concentrations of silver atoms in the vicinity of such a naked 8 nm particles will be much lower compared to the previous case, and therefore, the potential growth of a particle will be limited.

These results seem to apply to a rather general category of laser ablation processes in liquid phase. All colloidal particles undergoing post-irradiation will be completely or partially evaporated, depending on the size of the particle and the laser fluence. In the case of partial vaporization, they will lose their protective layer (for example, a surfactant layer), and then secondary particle growth will occur.

Finally, we can conclude that more detailed understanding of laser photolysis of silver colloid prepared using citric reduction method allows us to produce a relatively high concentration of small, spherical silver nanoparticles with a narrow size distribution. These 8 nm silver nanoparticles have a great potential for various applications and can be used as seeds in further synthesis processes.

Acknowledgment. Thanks to Dr. K. Lance Kelly for brief but very useful discussion.

References and Notes

- (1) Kreibig, U.; Vollmer, M. *Optical Properties of Metal Clusters*; Springer Series in Material Science 25; Springer: Berlin, 1995.
- (2) Kamat, P. V. *J. Phys. Chem. B* **2002**, *106*, 7729.
- (3) Kamat, P. V.; Flumiani, M.; Hartland, G. V. *J. Phys. Chem. B* **1998**, *102*, 3123.
- (4) Neddersen, J.; Chumanov, G.; Cotton, T. *Appl. Spectrosc.* **1993**, *47*, 1959.
- (5) Mafune, F.; Kohno, J.; Takeda, Y.; Kondow, T.; Sawabe, H. *J. Phys. Chem. B* **2000**, *104*, 9111.
- (6) Mafune, F.; Kohno, J.; Takeda, Y.; Kondow, T. *J. Phys. Chem. B* **2003**, *107*, 4218.
- (7) Pyatenko, A.; Shimokawa, K.; Yamaguchi, M.; Nishimura, O.; Suzuki, M. *Appl. Phys. A* **2004**, *79*, 803.
- (8) Takami, A.; Kurita, H.; Koda, S. *J. Phys. Chem. B* **1999**, *103*, 1226.
- (9) Lee, P. C.; Meisel, D. *J. Phys. Chem.* **1982**, *86*, 3391.
- (10) ASTM X-ray Powder Data File, Sets 1–5, **1960**.
- (11) Jensen, T.; Kelly, L.; Lazarides, A.; Schatz, G. C. *J. Cluster Sci.* **1999**, *10*, 295.
- (12) Kelly, L.; Jensen, T.; Lazarides, A.; Schatz, G. C. In *Metal Nanoparticles. Synthesis, Characterization, and Application*; Feldheim, D. L., Foss, C. A., Jr., Eds.; Dekker: New York, 2002.
- (13) *Perry's Chemical Engineers' Handbook*; Green D. W., Perry, R. H., Eds.; McGraw-Hill: New York, 1999.